High Time Resolution Measurements of Electron Temperature in a Laboratory Plasma

Vernon Chaplin[1], David Cohen[1], Michael Brown[1], and Chris Cothran[1,2]

1. Swarthmore College, Swarthmore, PA 19081 2. Haverford College, Haverford, PA 19041

Introduction

- The **Swarthmore Spheromak Experiment (SSX)** studies magnetic reconnection during the merging of two spheromaks:

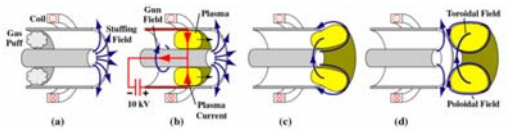

Figure 1. Schematic of **spheromak formation** in SSX. (a) Hydrogen gas is pumped into the space between the inner and outer electrodes, while current through the outer coils creates a "stuffing field." (b) The main capacitor banks discharge, ionizing the gas as a radial current flows from the outer to the inner electrode. (c) The **J × B** force between the gun field and the plasma current accelerates the spheromak out of the gun. (d) The plasma drags along the stuffing field, which reconnects to form the poloidal field of the spheromak. [Figure taken from J.Fung, Swarthmore College Honors Thesis, 2006]

- During **magnetic reconnection**, high magnetic field gradients cause field lines to change their topology and reconnect, converting stored magnetic energy into kinetic energy in bulk plasma flows or heating. This process provides a likely explanation for the extremely high temperatures observed in the solar corona, and has relevance in other astrophysical settings.

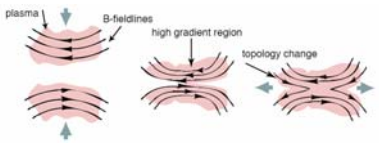

Figure 2. Magnetic reconnection. In a perfectly conducting plasma, magnetic field lines are "frozen-in" and move with the plasma. However, real plasmas have finite resistivity, so it is possible for field lines to diffuse through the plasma and reconnect. [Figure from Fung, 2006]

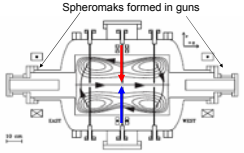

Figure 3. Lines of sight for VUV monochromator (red) and soft x-ray detector (blue) in SSX. [Figure from A. Falk, Swarthmore College Honors Thesis, 2003]

- In the SSX we study reconnection dynamics in several different merging configurations, focusing on the dynamics in the reconnection layer and how the annihilation of magnetic flux leads to flow, non-thermal particles, heating, and ultimately radiation. The spectral diagnostics discussed here are complemented by magnetic probe measurements, interferometric density diagnostics, and measurements from high-energy particle detectors.

Experimental Methods

- Probes inserted into the plasma can measure magnetic fields and provide information about bulk flows, but they also create significant perturbations in the plasma structure. **External, photon-based diagnostics** are therefore also useful for determining plasma properties.

- The SSX plasma is composed primarily of hydrogen. However, **impurity ions** from elements such as **carbon** and **oxygen** are also present in non-negligible quantities. Observations of emission from these ions provide a means for calculating plasma properties such as temperature and composition.

- Measurements were made using two complementary diagnostics:

  - Strengths of individual impurity emission lines were measured using a **vacuum ultraviolet (VUV) monochromator**.

  - In **coronal equilibrium** (validation discussed at top of next column) ionization balances and atomic level populations depend only on the plasma electron temperature (T_e), so observed line strength ratios can be used as a temperature diagnostic.

Figure 4. The SSX VUV monochromator.

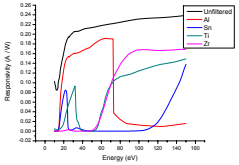

Figure 5. SXR filter response functions. The black line represents the responsivity of the unfiltered photodiodes.

- Broad spectral features were captured with the aid of a low resolution **soft x-ray detector (SXR)** composed of photodiodes filtered by thin films of Al, Ti, Sn, and Zr.

- Each SXR filter had a different **response function**, so the large-scale spectral dependence on T_e means that measured filter ratios can provide another temperature diagnostic.

- High (0.01 μs) time resolution allows temperatures to be calculated at 1 μs intervals.

Collisional-Radiative Modeling

- Extracting meaningful results from VUV monochromator and SXR data requires significant computational analysis.

- The non-LTE excitation kinematics code PrismSPECT was used to produce **model spectra** over a range of plasma conditions.

- **Time-dependent simulations** show that the plasma approaches a steady state ~10 μs after leaving the plasma gun (and well before reconnection, which occurs at about 40 μs).

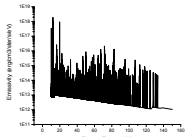

Figure 6. Spectrum produced for model with T = 44 eV and 0.1 % C, N, and O impurities present

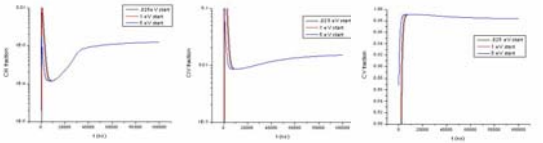

Figure 7. Time evolution of CIII, CIV, and CV fractions in simulations with T = 15 eV, nominal SSX density (8 x 10^{15} ions/cm^3 in the gun, decreasing linearly to 5 x 10^{14} ions/cm^3 at 30 μs), and starting atomic level populations calculated based on LTE at three different starting temperatures. The three simulations become nearly identical within 10 μs. The short time needed to reach equilibrium demonstrates that **steady-state simulations** are sufficient to achieve accurate results at SSX densities, and that the initial plasma conditions don't significantly affect the measurements we make at later times.

- VUV measurements of carbon emission line ratios averaged over many SSX shots were compared to results from steady-state simulations to calculate typical temperature profiles

- Model emission in each energy bin was multiplied by the SXR filter responsivities to determine simulated filter ratios. Results of a series of models were then compared to SXR measurements to determine a best-fit temperature profile for each shot

Results from the VUV Monochromator

- Impurity ion emission lines measured with VUV monochromator:

  - **CIII 97.7 nm** $1s^2 2s^1 2p^1\ ^1P_1 \rightarrow 1s^2 2s^2\ ^1S_0$
  - **CIV 155 nm** $1s^2 2p^1\ ^2P_{1/2}$ and $1s^2 2p^1\ ^2P_{3/2} \rightarrow 1s^2 2s^1\ ^2S_{1/2}$
  - **CIII 229.7 nm** $1s^2 2p^2\ ^1D_2 \rightarrow 1s^2 2s^1 2p^1\ ^1P_1$
  - **OV 63.0 nm** $1s^2 2s^1 2p^1\ ^1P_1 \rightarrow 1s^2 2s^2\ ^1S_0$
  - **NV 124 nm** $1s^2 2p^1\ ^2P_{1/2}$ and $1s^2 2p^1\ ^2P_{3/2} \rightarrow 1s^2 2s^1\ ^2S_{1/2}$

- Lines we failed to detect:

  - **CV 227.4 nm, OIV 55.4 nm, OIV 79 nm, OVI 103.5 nm, NIV 76.5 nm**

- Comparison of experimental results with simulations suggests that **carbon** is by far the dominant impurity in SSX, with smaller concentrations of oxygen and possibly nitrogen present.

- Further work is needed to place numerical constraints on impurity concentrations.

- The **CIII 229.7 line** was observed to be anomalously strong in experiments compared to its intensity in simulations at all plausible temperatures.

- The **CIII 97.7 nm / CIV 155 nm line ratio** proved to be extremely useful for calculating plasma electron temperatures.

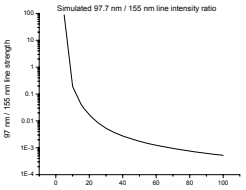

Figure 8. Temperature dependence of the CIII 97.7 nm / CIV 155 nm line intensity ratio calculated using steady-state PrismSPECT simulations.

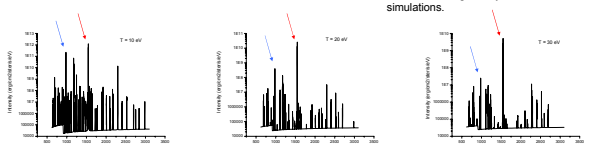

Figure 9. Sample PrismSPECT spectra for a 40 cm thick hydrogen plasma with 1% carbon impurity and T_e = 10 eV, 20 eV, and 30 eV (left to right). The CIV 155 nm and CIII 97.7 nm lines are the two strongest in all three simulations, but the relative strength of the 155 nm line increases as the plasma gets hotter and the carbon ionization balance shifts away from CIII and towards CIV.

- Preliminary results from temperature modeling using the CIII 97.7 nm / CIV 155 nm line ratio give an average plasma temperature of **25 eV** early in counter-helicity shots (at right), increasing to **35 eV** during magnetic reconnection (the counter-helicity configuration maximizes the amount of energy released during reconnection).

- Temperatures for single-spheromak shots (during which no reconnection took place) were approximately constant at **25 eV** (not shown).

- Further work will attempt to reduce the uncertainty in average temperature profiles caused by shot-to-shot variations in plasma structure.

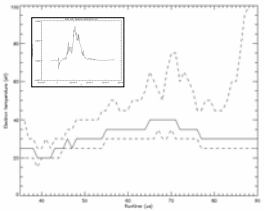

Figure 10. Electron temperature profile derived from the CIII 97.7 nm / CIV 155 nm line ratio averaged over 25 counter-helicity shots for each line. Dotted lines show the uncertainty range. The inset shows a sample VUV monochromator data trace (smoothed over 1 μs intervals).

Results from the Soft X-Ray Detector

- SXR temperature fitting was hindered by **anomalously strong signals** from the tin-filtered diode in nearly all experimental runs.

- Typical **tin (Sn)** signals were nearly twice as strong as Al signals and 5+ times stronger than Ti and Zr signals, a result that is hard to reconcile with Figure 5 for any reasonable spectrum.

- One solution to the mystery could be that the Sn filter passed significant photons at UV or visible wavelengths (E < 10 eV)

- A **"lollipop-like" device** was built to test this hypothesis.

- Measurements from a series of shots with the "lollipop" in place showed that less than 2% of the Sn filter signal was produced by UV or visible photons, thereby ruling out a UV leak as a significant cause of the anomalous results.

Figure 11. SXR lollipop device, featuring windows made of **UV-fused silica** (transmission cuts off abruptly above 7.3 eV), and **sapphire** (transmission cuts off above 8.3 eV). After the device was inserted into SSX, the windows were oriented at 90 degrees with respect to one another. Rotating the device then allowed us to position either window in the SXR line of sight.

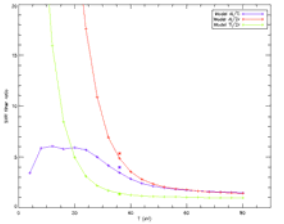

Figure 12. Example of SXR temperature fitting for a single time step during an SSX shot. Lines represent model-predicted filter ratios while lone points represent experimental data. Ratios involving the Sn filter have been omitted.

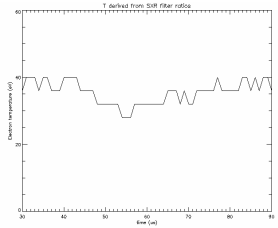

Figure 13. Best-fit temperature profile for a counter-helicity shot calculated from SXR data.

- Current results from SXR modeling with the Sn filter data omitted (see Figure 12) suggests an average electron temperature of ~40 eV during counter-helicity spheromak merging.

  - This value is within the uncertainty range for the average T_e calculated from VUV line ratios.

  - However, the expected spike in T_e during reconnection is not seen (Figure 13).

- It remains unclear whether we will be able to use SXR to derive reliable temperature estimates.

- Ongoing research is investigating the possibly that anomalous filter signals could be caused by **non-Maxwellian electron velocity distributions**.

Acknowledgements

This work was supported by the Department of Energy and the Research Corporation through grants to Swarthmore College, and by the Provost's office at Swarthmore College via a Tarble Summer Research Fellowship.

A copy of this poster can be found at http://astro.swarthmore.edu/~vchapli1/Files/Posters_and_Publications